Insolubilization and thermal stabilization of a long-chain polyester by non-catalyzed melt-polycondensation synthesis in air.

José Jesús Benítez[a,*], José Alejandro Heredia-Guerrero[b], Miguel Antonio Cruz-Carrillo[a], Markus Joachim Barthel[c], Heike Elisabeth Knicker[d] and Antonio Heredia[e].

[a] Instituto de Ciencia de Materiales de Sevilla (ICMS), Centro mixto CSIC-Universidad de Sevilla, Americo Vespucio 49, Isla de la Cartuja, 41092-Sevilla (Spain).
e-mail: benitez@icmse.csic.es
[b] Smart Materials, Department of Nanophysics, Fondazione Istituto Italiano di Tecnologia (IIT), via Morego 30, 16163 Genoa (Italy).
e-mail: Jose.Guerrero@iit.it
[c] Drug Discovery and Development Department, Fondazione Istituto Italiano di Tecnologia (IIT), via Morego 30, 16163 Genoa (Italy).
e-mail: Markus.Barthel@iit.it
[d] Departamento de Biogeoquímica, Ecología Vegetal y Microbiana, Instituto de Recursos Naturales y Agrobiología de Sevilla (IRNAS), CSIC, avda. Reina Mercedes 10, 41012 Sevilla (Spain).
e-mail: knicker@irnase.csic.es
[e] Departamento de Biología Molecular y Bioquímica, Universidad de Málaga, 29071 Málaga (Spain).
e-mail: heredia@uma.es

* Corresponding author

ABSTRACT

Self-standing films of poly(ω-hydroxyl hexadecanoic acid) (poly(ω-OHC16)) ***have*** been prepared by non-catalyzed melt-polycondensation in air at 150, 175 and 200°C. Poly(ω-OHC16)s obtained are characterized as polyesters by Infrared Spectroscopy (FT-IR) and Solid State Magic Angle Spinning ^{13}C Nuclear Magnetic Resonance (^{13}C MAS-NMR). Structurally, poly(ω-OHC16)s are quite crystalline as revealed by Wide Angle x-Ray Diffraction (WAXD). The presence of oxygen in the reaction atmosphere causes a mild oxidation in the form of peroxyester species, tentatively at the interphase between poly(ω-OHC16) crystallites, and the structure amorphization. The interfacial peroxyester phase ends up in the encapsulation of the polyester grains and provides a barrier towards the action of solvents. Thermal stabilization and insolubility resulting from the synthesis conditions used are interesting features to prepare solvent and heat resistant poly(ω-OHC16) coatings. Thus, a few microns thick poly(ω-OHC16) layer has been fabricated on aluminum foil and ***its resistivity towards a chloroform:methanol (1:1, v:v) mixture*** has been confirmed.

Keywords: long-chain polyester, thermoset, insoluble coating, melt-polycondensation.

INTRODUCTION

Research on bio-based polymeric materials has experienced an enormous impulse in the past few decades and future activity in this field is predicted to grow considerably.[1,2] The main motivations are the reduction on the dependence on non-renewable fossil fuel resources and the palliation of environmental damages associated to the production and post-use handling of fuel-based synthetic plastics.[3]

Among bio-based polymers, those obtained from cellulose, the most abundant biopolymer in nature, are the most widely studied.[4] Polyesters are another important group that can be obtained from abundant renewable resources like polysaccharides, vegetable oils and lignin.[5,6] Aliphatic polyesters became of interest because of their biocompatibility and biodegradability associated to the presence of the hydrolysable ester group. Poly(lactic acid) (PLA) and short-chain poly(hydroxyl alkanoates) (PHAs) like poly(3-hydroxybutyrate) (PHB) are good examples of successful renewable aliphatic polyesters with applications as biodegradable packaging and medical implants.[7] However, much less attention has been paid to mid and long-chain PHAs though poly(ω-hydroxyfatty acid)s poly(ω-OHFA)s are considered to be potential substitutes for polyethylene (PE) adding enhanced thermal stability, biodegradability and capabilities to form composite materials. [8,9] Two major reasons have been argued to justify such a low interest. First, the lack of practical and cost-effective routes to the obtaining of ω-hydroxyfatty acid monomers (ω-OHFAs) and second, the negative environmental and economic issues involving the organometallic catalysts used in the industrial polycondensation reaction.[10] Both problems seem to have been smoothed out when a commercially viable biotechnological route for the obtaining of ω-OHFAs[11] and the use of affordable and environmentally friendly titanium alkoxide catalysts were implemented.[10,12,13]

On the other side, and for certain biomedical applications, polymeric materials should be amorphous thermosets to retain its 3D structure and to provide a predictable loss of mechanical properties and a linear degradation at physiological conditions.[14] To develop facile

routes to elastomeric biomaterials, the thermal polyesterification without catalyst or coreagents has become a very attractive procedure.[15] Such methodology is also very suitable in fields like is the design of non-toxic protective coatings for food packaging, in which insoluble and infusible materials resisting the extended contact with foodstuff and the sterilization protocols are sought. To make the procedure even more attractive for a large scale production, we have also explored the potential of an easily scalable route consisting in the non-catalyzed polycondensation in molten state directly in air. [16] This method is different from the solid state polymerization (SSP),[17,18,19] because no pre-polymer is formed, the reaction temperature is above the melting point and no inert carrier or reduced pressure is used.

Thus, and connecting these issues, i.e. the regained interest in long chain poly(ω-OHFA)s, the convenience of biodegradable amorphous and insoluble thermosets for certain applications and the non-toxicity and economic advantages derived from the non-catalyzed one-step melt-polycondensation, we have studied the modifications of the physicochemical properties of a linear long chain poly(ω-hydroxyl hexadecanoic acid) prepared in air with particular attention to their thermal stability and ***resistivity*** to organic solvents. ***To address this later issue, we have used a mixture of chloroform and methanol, which has proven to be a very effective solvent for long-chain polyhydroxyalkanoates.***

EXPERIMENTAL

Materials

16-hydroxyhexadecanoic acid (>98.0%) was purchased from TCI and was used without further purification. Solvents (chloroform and methanol) were ACS-regent quality (Carlo Erba).

Polymer synthesis

Poly(ω-hydroxyl hexadecanoic acid) (poly(ω-OHC16)), were prepared by placing about 150 mg of 16-hydroxyhexadecanoic acid in an open carbon doped Teflon mold (35 mm x 10 mm and 0.5 mm deep) and heated inside an oven at 150, 175 and 200°C. The synthesis was carried out both in air (2 to 16 h), and under reduced pressure (16 h) using a diaphragm pump with a base pressure of 10 mm Hg. After cooling, self-standing films with about 350 µm thick were obtained.

Poly(ω-OHC16) coatings were made by spraying a chloroform:methanol (1:1, v:v) solution of 16-hydroxyhexadecanoic acid on a hot (~70°C) aluminum foil followed by heating in air for 30 minutes at 150 and 200°C. The thickness of the coating was estimated to be about 3 µm from gravimetric measurements.

Chemical and structural characterization

Infrared data were collected in a FT-IR spectrometer (FT/IR-6200, JASCO). For transmission IR measurements pellets containing about 2 mg of sample and 150 mg of dry KBr were used. Spectra were acquired by accumulating 32 scans using a TGS detector operated at 4 cm^{-1} resolution. Attenuated Total Reflected (ATR-FTIR) IR spectra were obtained from both sides of the films using a single reflection ATR accessory (MIRacle ATR, PIKE Technologies) coupled to a liquid nitrogen cooled MCT detector. All spectra were recorded in the 4000 to 600 cm^{-1} range at 4 cm^{-1} resolution and accumulating 50 scans.

The solid-state ^{13}C NMR spectra were acquired with a Bruker Avance III HD 400 MHz Wideboard operating at a frequency of 100.63 MHz using zirconium rotors of 4 mm OD with KEL-F-caps. The direct polarization technique was applied during magic-angle spinning of the rotor at 14 kHz. According to pre-experiments, a 30° ^{13}C pulse of 1.2 µs and a delay time of 40 s was enough to avoid signal saturation. 300 scans were accumulated and ^{13}C-chemical shifts were referred to tetramethylsilane at 0 ppm.

Wide-angle X-ray diffraction (WAXD) diffraction patterns were collected with an X'Pert Pro (PANalytical) diffractometer using monochromated CuK_{α} radiation and an X'Celerator detector with a 1/4° fixed slit. The diffractograms were recorded between 3 and 70° (2θ) in 0.0501° steps at 45 kV and 40 mA and 200 s counting time. The films were placed on a zero background silicon single crystal plate adapting them to the goniometer in a θ-2θ configuration. Crystalline indexes are calculated from the equation

$$CI = \frac{100 \times Ac}{Ac + Aa} \quad [1]$$

where *Ac* and *Aa* are the areas of the crystalline and amorphous peaks.[20]

Gel Permeation Chromatography (GPC) measurements were carried out using an Agilent 1260 Infinity quaternary LC system using two PLGel 5μm MIXED-C columns at 25°C and a refractive index detector. Dimethyl formamide (DMF) was used to dissolve poly(ω-OHC16) samples and as eluent at 1 mL/min flow rate. The system was calibrated with Agilent EasyVial PS standards. Only the series prepared at 150°C was soluble enough to allow GPC analysis.

Thermal analysis

Differential Scanning Calorimetry (DSC) thermograms were acquired with a DSC Q20 (TA Instruments) from -70 to 150°C under nitrogen flow (50 mL/min) at 10°C/min using non-hermetic aluminum pans. Circular pieces of the films (~4 mg) were cut and placed in good contact with the bottom of the pan. The glass transition temperature (T_g) was obtained using the inflection method.

The thermal stability of samples was monitored by means of Thermal Gravimetric Analysis (TGA) with a SDT Q600 TGA/DSC analyzer (TA Instruments). Specimen (~10 mg) were heated from RT to 500°C at 5°C/min under either N_2 or synthetic air flow (100 mL/min).

Mechanical characterization

Tensile tests of films were carried out using an MTS Criterion 42 machine equipped with a 50 N load cell and applying a 0.02 N preload. Rectangular uniform pieces (7 mm x 30 mm) and typically 350 μm thick were cut and brought to rupture at a constant deformation rate of 0.2 mm/min at room environmental conditions. Stress values were calculated using the specimen cross-section under no applied load. The Young´s modulus was obtained from the slope of the stress-strain curve within the first 1-4% strain range using the built-in software. Experiments were repeated at least 5 times and parameters averaged to ensure reproducibility.

Solubility assays

Sample solubility was tested in pure solvents such as chloroform, methanol, ethanol, tetrahydrofuran, toluene and dimethyl sulfoxide. Best results were obtained with chloroform. When using this solvent, the solubility was further increased with the addition of an equivalent amount of methanol, likely because of the combination of the chloroform affinity for the aliphatic fraction and that of methanol for the polar and hydrogen bonding –OH, -COOH and ester groups. Thus, the chloroform:methanol (1:1, v:v) mixture was chosen as the most suitable for the solubility tests.

Insoluble fraction was then calculated by measuring the weight loss of minced samples (about 150 mg) placed inside a glass microfiber extraction thimbles immersed in a chloroform:methanol (1:1, v:v) mixture at 40°C for 96 h under agitation.

The solvent ***resistivity*** of coatings was tested by immersing one half of the coated Al foil in a chloroform:methanol (1:1, v:v) solution at room temperature for 12 h without agitation.

Surface hydrophobicity

Static Water Contact Angle (WCA) of films and coatings were determined with an Attension TL100 Optical Tensiometer by the sessile drop method and image profile analysis. A 3 μL Milli-Q grade water drop was deposited in at least 5 different points of every sample and the drop contour was recorded. Values reported correspond to the average of about 20 stable measurements within the first 5 seconds of contact.

RESULTS AND DISCUSSION

Chemical characterization

The self-esterification of the ***ω-OHC16*** acid has been monitored by transmission IR spectroscopy up to 16 h reaction at 150, 175 and 200°C, Figure 1. Final products are characterized as polyesters by intense peaks at 1736 and 1174 cm^{-1} corresponding to C=O and C-O stretching modes,[21,22] respectively (full spectra are shown in Figure S1 in supporting information). Compared to samples prepared under reduced pressure, those synthesized in air display a more complex carbonyl region. Thus, in addition to the main 1736 cm^{-1} peak, others at 1775, 1713 and 1696 cm^{-1} are observed. The weak shoulder at 1696 cm^{-1} is due to unreacted 16-hydroxyhexadecanoic acid molecules. The assignation of the 1713 cm^{-1} band is not straightforward: its parallel evolution with the 1696 cm^{-1} shoulder supports the adscription to free acid groups in a less associated form or in oligomeric units.[23,24] However, the contribution of carbonyl ester groups perturbed by hydrogen bonding with such free acid molecules or even with trapped residual water molecules cannot be ruled out.[25]

The band at 1775 cm^{-1} is only visible in samples prepared in air and its intensity increases with temperature and reaction time, consequently, it is related to oxidation by-products. The generation of the anhydride (R-(CO)-O-(CO)-R´) and the per-acid (R-(CO)-O-O-H) are discarded because no chemical modification has been observed at 150 and 175°C for pure poly(hexadecanedioic acid) under the same preparation conditions (see Figure S2 in Supporting Information). The formation of the diacyl peroxide (R-(CO)-O-O-(CO)-R´) can also be

ruled out because it would give rise to a second band 25 cm^{-1} above the one at 1775 cm^{-1}.[21] Then, and considering the 39 cm^{-1} increment from the ester frequency, the more plausible hypothesis is the formation of a peroxyester (R-(CO)-O-O-R´).[26,27]

At 200°C the range of oxidized species may expands. Thus, the formation of the anhydride (characterized by two absorptions around 1775 and 1715 cm^{-1}) is now possible, as observed for the reference poly(hexanedioic acid) (Figure S2 in Supporting Information). Furthermore, the broadening of the carbonyl band, particularly at the high wavenumber side, can be due to the additional contribution of the diacyl peroxide (typical doublet doublet at 1786 and 1812 cm^{-1}).[26]

Solid state ^{13}C NMR data, Figure 2, support IR results. The formation of the corresponding esters by heating in air is corroborated by peaks at 173 and 64.2 ppm.[10,28] The presence of free -COOH groups can also be detected by the signal around 180.5 ppm. The amount of acid is estimated to range from 11% at 150°C to 8% at 200°C. However, such acid peak is not accompanied by a comparable free hydroxyl signal around 62 ppm. The same is observed in the ^{13}C NMR spectrum of the solubilized sample prepared at 150°C (Figure S3 in supporting information). This result indicates that –COOH groups detected are not only due to residual unreacted 16-hydroxyhexadecanoic acid molecules, but also to the oxidation of a small amount of primary hydroxyls before undergoing esterification.

Solid state ^{13}C NMR also displays a sharp peak in the 176.5-177.0 ppm range which is not observed when the polyester is prepared under reduced pressure. Such peak is located between those of the acid and the ester carbonyls and it is assigned to a peroxyester by-product resulting from the side oxidation reaction (Figure S4 in Supporting Information).[29] This assignation is supported by another peak at 73 ppm corresponding to the aliphatic carbon contiguous to the peroxy group. As observed in IR spectra, the carbonyl ^{13}C NMR peak becomes broader as the synthesis temperature is raised, which is considered to be the result of the aforementioned contribution of other residual oxidized species.

Crystallinity of poly(ω-OHC16)s

Wide-angle X-ray diffraction (WAXD) data shows that polyesters prepared from 16-hydroxyhexadecanoic acid by melt-polycondensation under reduced pressure are quite crystalline (see Figure S5 in Supporting Information). ***Calculated crystalline index (CI) values are 83.0, 82.7 and 77.9% after 16h reaction at 150, 175 and 200°C, respectively.*** Additional spectroscopic features confirm such observation. Among them: the splitting of $-CH_2-$ deformation bands at 1468 cm^{-1} (scissoring) and 724 cm^{-1} (rocking),[30] the series of equally spaced peaks in the 1430-875 cm^{-1} range (see Figure S1 in Supporting Information)[31] and the solid state ^{13}C NMR peak at 32.4 ppm corresponding to skeleton methylene groups in all-trans configuration.[32,33]

When the synthesis is carried out in air, Figure 3A, the same sharp WAXD peaks at 2θ = 21.34, 23.70, 29.78, 35.99 and 40.30° corresponding to *d*-spacings of 4.16, 3.75, 3.00, 2.49 and 2.24 Å of the (1 1 0), (2 0 0), (2 1 0), (0 2 0) and (3 1 0) planes of the orthorhombic methylene subcell packing,[34] respectively, are also observed. Additionally, an amorphous phase (α, broad peak ~20°) progressively develops as the temperature and reaction time are increased. Such amorphization is monitored by the parameter (α), which is calculated as (100-*CI*) where *CI* is the crystalline index as defined in equation 1. As observed, (α) values progressively grows with reaction time and temperature and reach a plateau between 20 and 60%, Figure 3B. ***Under reduced pressure, final (α) values are much smaller and range between 17% at 150°C and 22.1% at 200°C. The small increment upon heating is very likely due to the enhancement of side oxidations caused by traces of oxygen in the reaction atmosphere used (10 mm Hg base pressure).***

Poly *(*ω-OHC16*)* obtained under reduced pressure displays a sharp melting peak at 94°C with ΔH_m = 153 J/g, Figure 4. When samples are prepared in air, the melting peak progressively diminishes, broadens and displaces to lower temperature as the reaction time and

temperature are increased. This result evidences the degradation of chain packing and the reduction of long-range order. Meanwhile, the apparition of a glass transition around -15°C characterizes the formation of the amorphous phase. Figure 4 also shows that there is a good correlation between the diminishment of the melting enthalpy and the amorphization of poly(ω-OHC16).

Solubility and structure

While poly(ω-OHC16) prepared at 150°C was found to be soluble in a chloroform:MeOH (1:1, v:v) mixture, the solubility of the 175 and the 200°C series decreased very drastically as the reaction time was increased, table 1 and Figure S6 in Supporting Information. For this reason, GPC analysis was only possible for samples prepared at 150°C. Compared to reported results for poly(ω-OHC14) synthesized by the catalyzed route in solution,[10] polymeric chain sizes obtained in the self-polycondensation in molten state are quite small and display a very broad distribution, table 1. Calculated weight average molecular weights (Mw) increased linearly with reaction time until stabilization above 8 h. These results suggest the prevalence of a chain-growth rather than a step polymerization mechanism at the preparation conditions used. Thus, in a first stage, the hydroxyacid molecules would react to form low molecular weight ensembles until the progressive increment of the viscosity of the medium reduces diffusion and hinders the further incorporation of monomers and oligomers. There is no reason to expect a substantial modification of this mechanism by increasing the temperature and thus the formation of high Mw moieties justifying the strong solubility reduction in the 175 and the 200°C series is ruled out.

In molten state and in contact with air, poly(ω-OHC16) formed gets partially oxidized. When cooled down, linear polymeric chains rearrange into crystalline domains, but the presence of peroxy groups arising from oxidation introduces a lattice mismatch that truncates the process and leads to the formation of an amorphous phase separating the crystalline

regions. Figure 5 shows that insolubility is directly correlated with such amorphous phase as calculated from ***XRD***. However, the quantitative analysis of IR and ^{13}C NMR data demonstrates that the formation of a pure and segregated peroxyester phase itself is not enough to account for the insoluble fractions measured. For instance, the maximum amount of peroxyester groups detected is about 25% while the corresponding insoluble fraction is 81.2%. To address the question about why such a moderate oxidized phase causes such a strong insolubility, we propose a decorating effect in which the peroxyester phase encapsulates amorphous and/or crystalline moieties of the polyester and prevents the solvent attack, Figure 5. At low oxidation degree, either encapsulation is not fully completed or particles are too small and migrate to the solvent forming a suspension. For that reason the 150°C series shows almost full solubility despite the moderate amorphous fraction detected.

Near surface modification by polycondensation in air

To further investigate the effect of air induced peroxidation on the structure and properties of poly(ω-OHC16), we have used a near surface sensitive IR technique like ATR-FTIR. In the experimental configuration employed, the ATR-FTIR spectra of ν(C=O) provides information from about a 2.5 µm deep region from the incidence side. Thus, the near surface alteration of both: the air exposed (top) and the air preserved (bottom) sides of the poly(ω-OHC16) film can be independently studied.

Spectra in Figure 6A ***and in Figure S1 in Supporting Information***, show that, in the temperature range studied, the near surface region of the air preserved side (bottom part) is ***very similar to the bulk. It is a quite*** crystalline region and contains very little oxidation by-products. On the opposite face, and in the presence of oxygen, surface oxidation and amorphization are considerable. The evolution of the peroxyester band in both sides, as a function of temperature and reaction time, is displayed in figure 6B. As expected, the oxidation is much more intense on the air exposed side and the low peroxyester content at the air

preserved face evidences the low diffusion of oxygen through molten poly(ω-OHC16) bulk. ~~***It is also remarkable the strong surface oxidation at 200°C***~~. ***Therefore, oxidation seems to be restricted to the near surface regions of the film***.

On the other hand, ***it is difficult to obtain*** cross-sectional structural data on these films. However, when analyzing bulk properties, we did find a good correlation between the width of the $\nu_{sym}(-CH_2-)$ IR peak and the amorphous content (α), Figure 3C. ***We have transferred such correlation to the near surface region analysis*** and we consider this parameter to be a suitable indicator ***for*** crystallinity. We have used it to verify the direct relationship between the formation of oxidized species and the amorphization process ***in the near surface regions of poly(ω-OHC16) films***, Figure 6C.

Mechanical performances of poly(ω-OHC16)

Semi logarithmic stress-strain curves of the series of poly(ω-OHC16) obtained in air are displayed in Figure 7. As a reference, samples prepared at 150°C under reduced pressure are brittle with Young´s modulus values around 200 MPa and small fracture strains (~6%). When synthesized in air, the brittle behavior is retained though a reduction of the Young´s modulus (~150 MPa) and the stress at break (UTS) are observed.

As the preparation temperature and time are raised, the films become more ductile and yield points and strain softening regions are observed.[35] Crystallinity has been proposed as one of the main factors affecting the tensile parameters of polymers, hence the amorphization of the polyester structure is considered to be responsible for such a brittle to ductile transition. Amorphous regions connecting rigid crystallites withstand high elongations and confer plasticity. Thus, the progressive diminution of the Young´s modulus and the stress at break in the 175°C series are accompanied by the increment of the strain at break. The 200°C series follows the same pattern, i. e. a modulus and UTS reduction, but, surprisingly, it shows very little modification of elongation at break values. To account for this observation, ATR-FTIR data

are analyzed (Figures 6B and 6C). They reveal an intense amorphization and accumulation of oxidized species at the air-exposed near surface region of samples prepared at 200°C. In this case, we propose a breaking mechanism in which the fracture is initiated at this altered near surface region and then propagated towards the bulk allowing little elongation.

Thermal stability

The thermal degradation of poly (ω-OHC16) is a single step process initiated by the random scission of the C-O bond of the ester group and followed by the fast fragmentation of generated carboxyl (R-(CO)-O•) and alkyl (•R´) radicals.[36] Maximum weight loss rates ($T_{d\ max}$) are around 410°C and do not depend on the atmosphere used for their preparation, table 2. The onset degradation temperature ($T_{d\ 5\%}$) is defined as the temperature at which the initial 5% weight loss is detected and it constitutes a critical value characterizing the thermal stability of polymers. $T_{d\ 5\%}$ values for the series prepared under reduced pressure are about 380 °C and agrees with values reported for other poly(ω-OHFAs).[37] For the specimen prepared in air, the onset degradation temperatures decrease about 65°C, very likely due to the cleavage of the more labile O-O bond of the peroxy species formed in such conditions.[36] Thus, the primary scission of the peroxyester gives rise to new alkoxy radicals (R-O•) following a different fragmentation pattern and ending up in a permanent carbon char residue that grows with the reaction temperature used, table 2. In the presence of oxygen, the thermal stability of poly(ω-OHC16) decreases. Measured $T_{d\ 5\%}$ are 20 to 40°C lower and the carbonaceous build up grows, probably because of the formation of extra (R-O•) species from alkyl (R•) radicals.

Coatings of poly(ω-OHC16)

Data presented in the previous paragraphs show that conducting the self-polycondensation reaction in air confers new properties like insolubility and infusibility to poly(ω-OHC16). These are valuable features, for instance, to prepare thermally stable and

solvent resistant coatings. To explore the potential of such methodology, we have created a few microns (3µm) thick layer of poly(ω-OHC16) on aluminum foil by curing in air a sprayed deposit from a ***ω-OHC16*** solution. Images in Figure 8 correspond to heating at 150 and 200°C for 30 minutes. In both cases, ATR-FTIR spectra reveal the formation of the ester by characteristic peaks at 1730 and 1170 cm^{-1} though some oxidation is also observed at 200°C by means of the shoulder at 1775 cm^{-1}. Both layers are structurally different; the splitting of the methylene deformation bands at 1468 and 727 cm^{-1}, as well as the series of periodic absorptions in the 1400-900 cm^{-1}, indicate that the coating prepared at 150°C is quite crystalline while the one obtained at 200°C is mostly amorphous. When exposed to an aggressive solvent like a chloroform:methanol (1:1, v:v) mixture, the coating prepared at 150°C is completely washed out while the one at 200°C remains virtually unaltered. Thus, the synthesis in air of poly(ω-OHC16) allows the obtaining of an insoluble coating showing a remarkable thermal stability and an acceptable surface hydrophobicity, table 2.

More work is needed to establish the optimal preparation parameters and to complete the characterization of these coatings (mechanical properties, permeability, transparency, wear resistance, etc…), but, in this preliminary study, we have shown that few micron thick coating of poly(ω-OHC16) prepared by non-catalyzed melt-polycondensation in air do retain essential properties of thicker films.

CONCLUSIONS

Fatty polyester poly(ω-OHC16) self-standing films can be prepared from 16-hydroxyhexadecanoic acid by non-catalyzed melt-polycondensation in air. Though molecular weights achieved are much lower than those obtained by catalyzed two-stage polymerizations, the amorphization induced by oxidation side reactions entail the modification of their physical properties. Solids become more plastic, insoluble and infusible, which is of interest, for instance, to create thermally stable and solvent resistant coatings from fatty ω-hydroxyacid by

a direct and easily scalable method using no potential hazardous agents like solvents and metal catalysts.

ACKNOWLEDGEMENTS

Funding is provided by the Andalusian Regional Government (Junta de Andalucía grant TEP-7418). JAH-G acknowledges the BIOPROTO project (Marie Curie Intra-European Fellowship), financed by the EU Seventh Framework Programme for Research (FP7). MAC-C is a post-doctoral grant holder from the CONACYT (Mexico) mobility program.

	Mw (g/mol)	PDI	Insoluble fraction (%)		
Reaction time (h)	150 °C		150 °C	175 °C	200 °C
2	2290	1.83	0.6	4.6	44.9
4	7870	3.77	0.1	21.9	64.9
6	12600	5.25	-0.2	43.2	72.1
8	17600	7.18	-0.3	53.2	74.5
10	16800	7.15	0.3	60.1	77.3
12	20200	6.85	1.9	64.2	79.1
14	21450	8.03	2.8	67.8	81.2
16	19450	7.63	4.1	71.0	81.2

Table 1. Weight average molecular weight (Mw), polydispersity (PDI) and insoluble fraction values of poly(ω-OHC16) prepared in air.

	TGA (in N_2)						TGA (in air)			WCA (°)		
Reaction atmosphere	Reduced pressure			Air			Air			Reduced pressure	Air	Air
Reaction temperature (°C)	$T_{d\ max}$ (°C)	$T_{d\ 5\%}$ (°C)	Residue (%)	$T_{d\ max}$ (°C)	$T_{d\ 5\%}$ (°C)	Residue (%)	$T_{d\ max}$ (°C)	$T_{d\ 5\%}$ (°C)	Residue (%)	Film		Coating
150	411	380	0.9	403	314	3.5	415	291	9.5	84	83	78
175	414	385	0.7	410	315	7.2	411	287	16.5	83	81	75
200	408	373	0.8	409	318	11.9	413	277	18.0	84	84	76

Table 2. Thermogravimetric (TGA) and static water contact angle (WCA) data for poly(ω-OHC16) synthesized for 16 h.

FIGURE CAPTIONS

Figure 1. Transmission IR-FTIR spectra of the (C=O) region of poly(ω-hydroxyl hexadecanoic acid) prepared by non-catalyzed melt-polycondesantion at 150, 175 and 200°C for reaction times ranging from 2 to 16 h in air and 16 h under reduced pressure. The formation of oxidized species is monitored by normalizing the area of the broad band at 1775 cm^{-1}.

Figure 2. Single-pulse solid state ^{13}C NMR MAS of poly(ω-OHC16) obtained for 16 h at the indicated temperature and atmosphere. The intensity of the 225-50 ppm is expanded by a factor of 3.

Figure 3. (A) Wide-angle X-ray diffraction (WAXD) patterns of poly(ω-OHC16) prepared at 150, 175 and 200°C for 16 h in air. (B) Quantification of the amorphous phase (α) formed as a function of temperature and reaction time. (C) Empirical relationship found between the percentage of crystallinity and the width of the symmetrical ($-CH_2-$) stretching IR band of poly(ω-OHC16).

Figure 4. Differential Scanning Calorimetry (DSC) thermograms of poly(ω-OHC16) prepared for 16 h at the indicated temperature and atmosphere. The development of an amorphous phase is evidenced by a glass transition (T_g). Melting enthalpies (ΔH_m) of the series were found to decrease with the progression of the amorphous phase.

Figure 5. Relationship between the development of the amorphous phase and the reduction of solubility of poly(ω-OHC16) prepared in air. The model proposes the formation of an oxidized phase shielding the polyester and preventing the solvent attack.

Figure 6. (A) Attenuated Total Reflected (ATR-FTIR) IR spectra of both sides of poly(ω-OHC16) films prepared in air at 150, 175 and 200°C for 16 h. Contact with air has a strong influence on the chemical composition (B) and crystallinity of the near surface region (C).

Figure 7. Uniaxial tensile parameters and semi-logarithmic stress-strain curves of poly(ω-OHC16) prepared in air at the indicated temperature and reaction time. Samples within the colored region show a yield point.

Figure 8. Poly(ω-OHC16) coatings (~3 µm thick) on aluminum foil fabricated from a sprayed 16-hydroxyhexadecanoic acid deposit by heating in air at 150 and 200°C for 30 minutes. Immersion in a chloroform:methanol (1:1, v:v) mixture removes the layer prepared at 150°C but does not affect the one obtained at 200°C.

Figure 1.

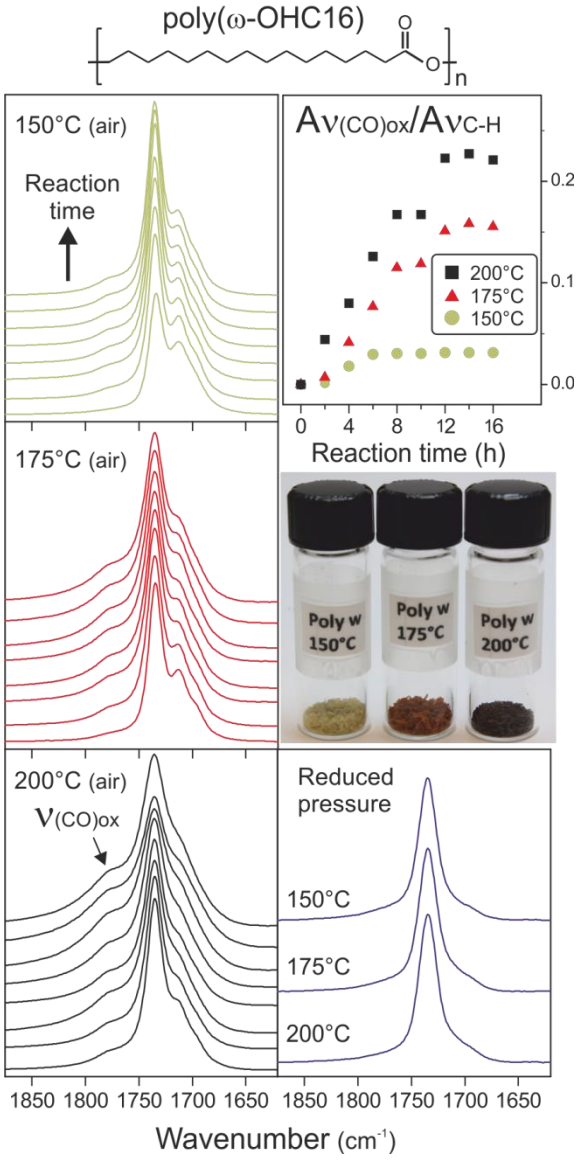
poly(ω-OHC16)
150°C (air)
Reaction time
175°C (air)
200°C (air)
ν(CO)ox
Aν(CO)ox/AνC-H
200°C
175°C
150°C
0.2
0.1
0.0
0 4 8 12 16
Reaction time (h)
Poly w 150°C
Poly w 175°C
Poly w 200°C
Reduced pressure
150°C
175°C
200°C
1850 1800 1750 1700 1650 1850 1800 1750 1700 1650
Wavenumber (cm-1)

Figure 2.

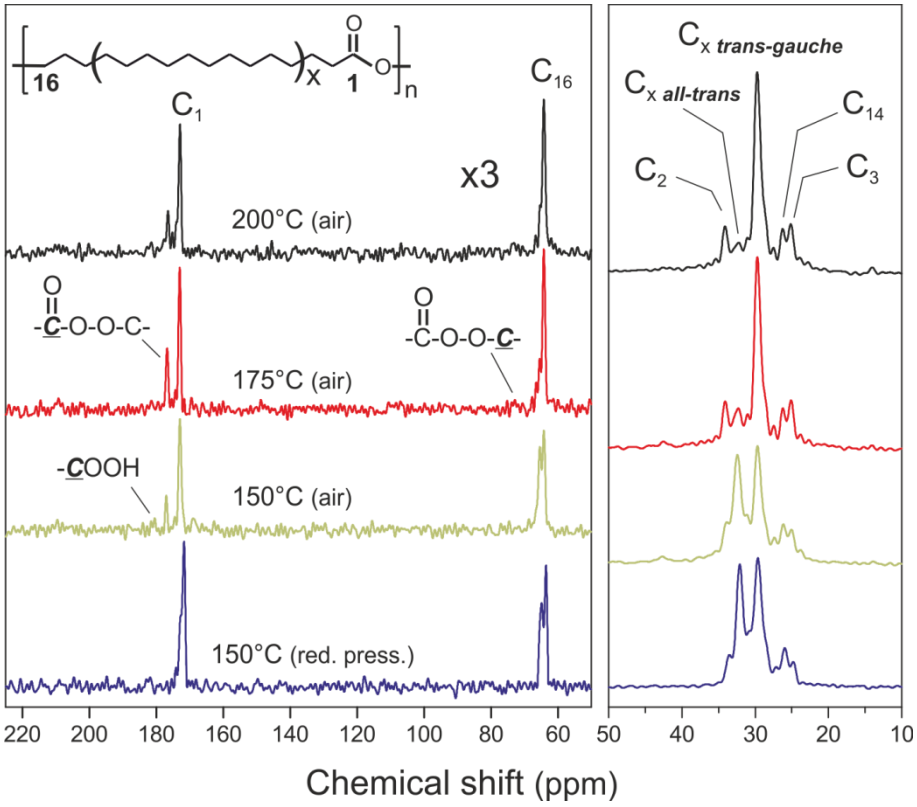
16
x
1
n
C1
C16
x3
200°C (air)
-C-O-O-C-
-C-O-O-C-
175°C (air)
-COOH
150°C (air)
150°C (red. press.)
Cx trans-gauche
Cx all-trans
C14
C2
C3
220
200
180
160
140
120
100
80
60
50
40
30
20
10
Chemical shift (ppm)

Figure 3.

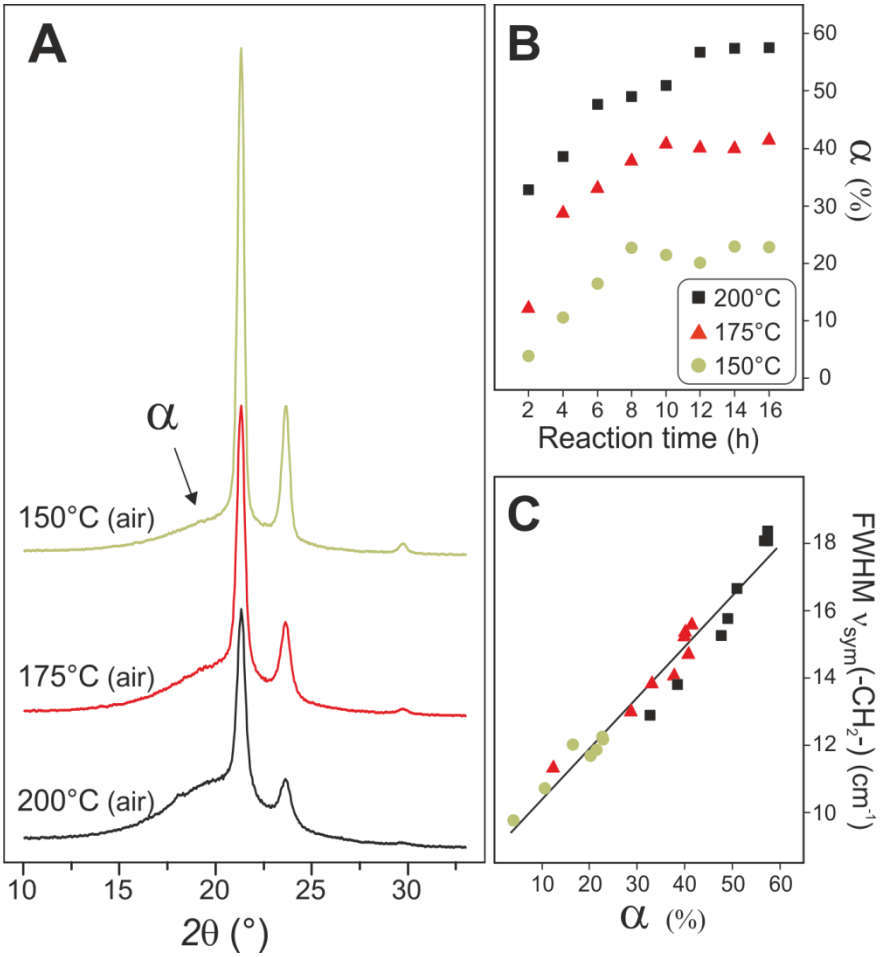
A
α
150°C (air)
175°C (air)
200°C (air)
10
15
20
25
30
2θ (°)
B
60
50
40
30
20
10
0
α (%)
200°C
175°C
150°C
2
4
6
8
10
12
14
16
Reaction time (h)
C
18
16
14
12
10
FWHM ν_sym(-CH2-) (cm-1)
10
20
30
40
50
60
α (%)

Figure 4.

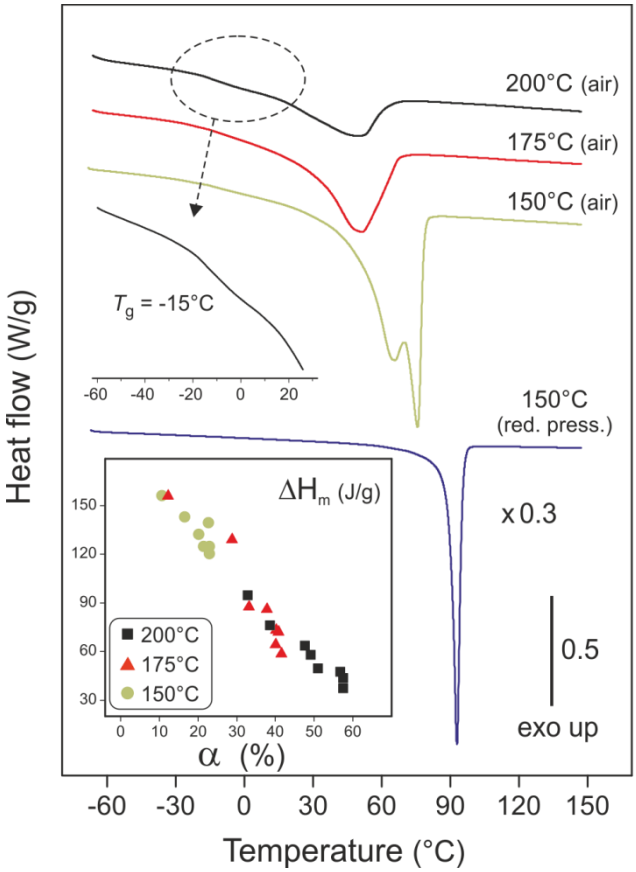
200°C (air)
175°C (air)
150°C (air)
T_g = -15°C
-60 -40 -20 0 20
150°C
(red. press.)
x 0.3
0.5
exo up
ΔH$_m$ (J/g)
150
120
90
60
30
200°C
175°C
150°C
0 10 20 30 40 50 60
α (%)
Heat flow (W/g)
-60 -30 0 30 60 90 120 150
Temperature (°C)

Figure 5.

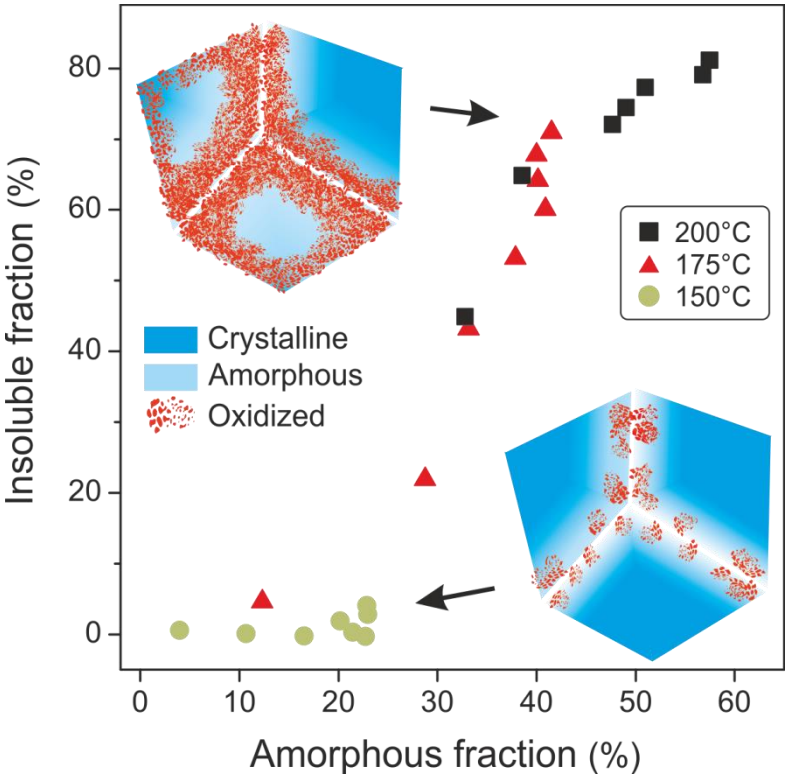
Insoluble fraction (%)
Amorphous fraction (%)
0
20
40
60
80
0
10
20
30
40
50
60
200°C
175°C
150°C
Crystalline
Amorphous
Oxidized

Figure 6.

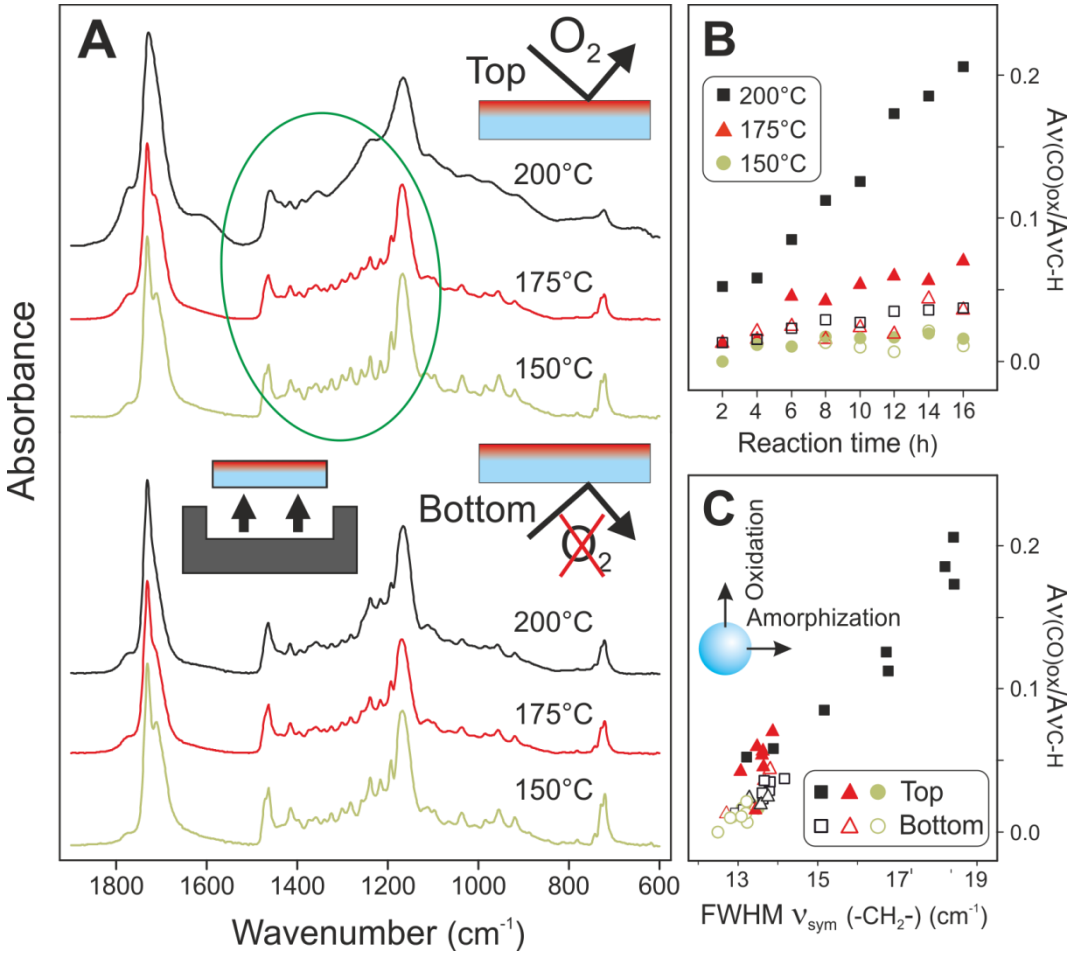
A
Top
O_2
200°C
175°C
150°C
Bottom
O_2
200°C
175°C
150°C
Absorbance
1800
1600
1400
1200
1000
800
600
Wavenumber (cm^{-1})
B
200°C
175°C
150°C
0.2
0.1
0.0
Av(CO)ox/Av(C-H)
2
4
6
8
10
12
14
16
Reaction time (h)
C
Oxidation
Amorphization
Top
Bottom
0.2
0.1
0.0
Av(CO)ox/Av(C-H)
13
15
17
19
FWHM ν_{sym} (-CH$_2$-) (cm^{-1})

Figure 7.

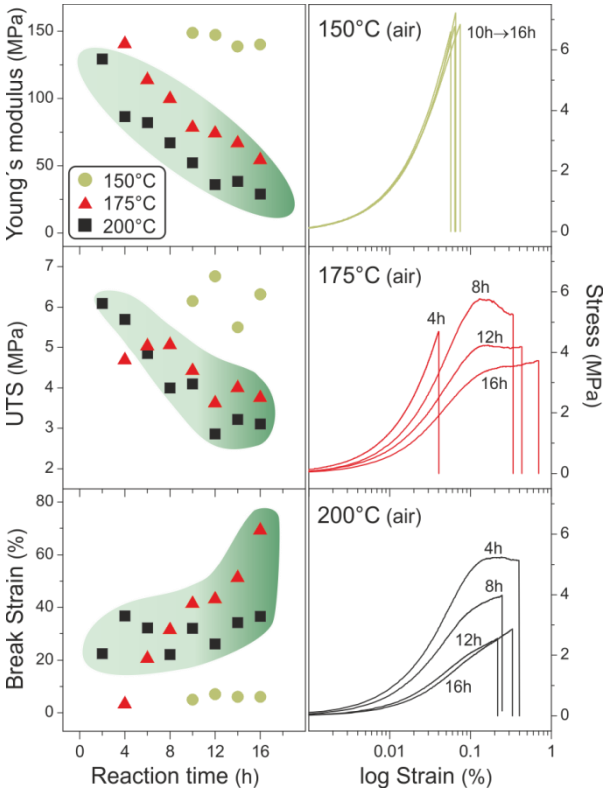
Young´s modulus (MPa)
UTS (MPa)
Break Strain (%)
Reaction time (h)
150°C
175°C
200°C
150°C (air)
10h→16h
175°C (air)
4h
8h
12h
16h
200°C (air)
4h
8h
12h
16h
Stress (MPa)
log Strain (%)

Figure 8.

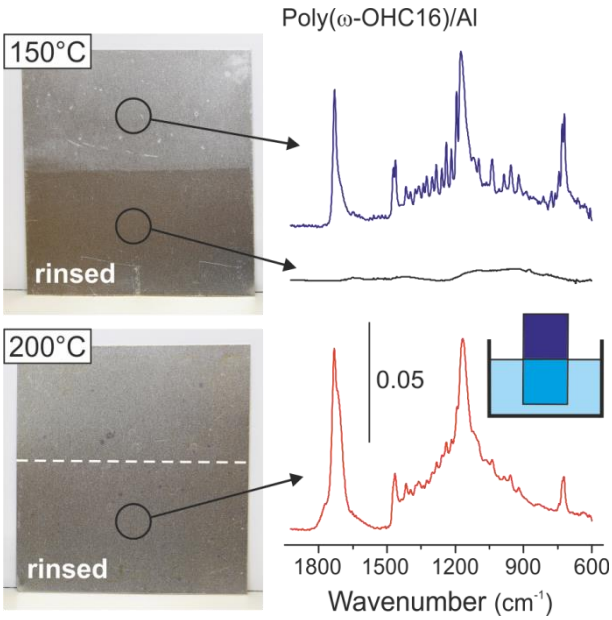
Poly(ω-OHC16)/Al
150°C
rinsed
200°C
rinsed
0.05
1800
1500
1200
900
600
Wavenumber (cm-1)

Graphical abstract

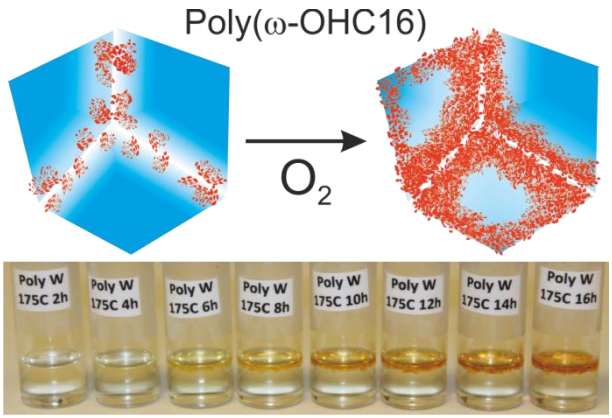

REFERENCES

1. Shen, L.; Worrell, E.; Patel, M. *Biofuels, Bioprod. Biorefin.* **2010**, *6*, 25.

2. Chen, G. Q.; Patel, M.K. *Chem. Rev.* **2012**, *112*, 2082.

3. Lithner, D.; Larsson, A.; Dave, G. *Sci. Total Environ.* **2011**, *409*, 3309.

4. Klemm, D.; Heublein, B.; Fink, H. P.; Bohn, A. *Angew. Chem. Int. Ed.* **2005**, *44*, 3358.

5. Vilela, C.; Sousa, A. F.; Fonseca, A. C.; Serra, A. C.; Coelho, J. F. J.; Freire, C. S. R.; Silvestre, A. J. D. *Polym. Chem.* **2014**, *5*, 3119.

6. Quinzler, D.; Mecking, S. *Angew. Chem. Int. Ed.* **2010**, *49*, 4306.

7. Chen, G. Q. *Chem. Soc. Rev.* **2009**, *38*, 2434.

8. Cole-Hamilton, D. J. *Angew. Chem. Int. Ed.* **2010**, *49*, 8564.

9. Petrović, Z. S.; Milić, J.; Xu, Y.; Cvetković, I. *Macromolecules* **2010**, *43*, 4120.

10. Liu, C.; Liu, F.; Cai, J.; Xie, W.; Long, T. E.; Turner, S.R.; Lyons, A.; Gross, R. A. *Biomacromolecules* **2011**, *12*, 3291.

11. Lu, W.; Ness, J. E.; Xie, W.; Zhang, X.; Minshull, J.; Gross, R. A. *J. Am. Chem. Soc.* **2010**, *132*, 15451.

12. Shirahama, H.; Kawaguchi, Y.; Aludin, M. S.; Yasuda, H. *J. Appl. Polym. Sci.* **2001**, *80*, 340.

13. Jose, J.; Pourfallah, G.; Merkley, D.; Li, S.; Bouzidi, L; Leao, A. L.; Narine, S. S. *Polym. Chem.* **2014**, *5*, 3203.

14. Amsden, B. *Soft Matter.* **2007**, *3*, 1335.

15. Barrett, D. G.; Merkel, T. J.; Luft, J. C.; Yousaf, M. N. *Macromolecules* **2010**, *43*, 9660.

16. Benítez, J. J.; Heredia-Guerrero, J. A.; Guzmán-Puyol, S.; Barthel, M. J.; Domínguez, E.; Heredia, A. *Front. Mater.* **2015**, *2:59*, 1.

17. Fortunato, B.; Pilati, F.; Manaresi, P. *Polymer* **1981**, *22*, 655.

18. Moon, S. I.; Lee, C. W.; Taniguchi, I.; Miyamoto, M.; Kimura, Y. *Polymer* **2001**, *42*, 5059.

19. Gupta, A. P.; Kumar, V. *Eur. Polym. J.* **2007**, *43*, 4053.

20. Murthy, N. S.; Minor, H. *Polymers* **1990**, *31*, 996.

21. Bellamy, L. J. In The infrared spectra of complex molecules; Chapman and Hall: London, **1975**; p. 203.

22. Noda, I.; Dowrey, A. E.; Haynes, J. L.; Marcott, C. In Physical Properties of Polymers Handbook, J.E. Mark (Ed.); Springer Science+Business Media: New York, **2007**; p. 395.

23. Maréchal, Y.; Chamel, A. *J. Phys. Chem.* **1996**, *100*, 8551.

24. Dong, J.; Ozaki, Y.; Nakashima, K. *Macromolecules* **1997**, *30*, 1111.

25. Ramirez, F. J.; Luque, P.; Heredia, A.; Bukovac, M. J. *Biopolymers* **1992**, *32*, 1425.

26. Davison, W. H. T. *J. Chem. Soc.* **1951**, 2456.

27. Pabin-Szafko, B.; Wisniewska, E.; Hefczyc, B.; Zawadiak, J. *Eur. Polym. J.* **2009**, *45*, 1476.

28. Saam, J. C. *J. Polym. Sci., Part A: Polym. Chem.* **1998**, *36*, 341.

29. ChemDraw Professional 15.0.0.106 software, PerkinElmer Informatics Inc.

30. Hagemann, H.; Snyder, R. G.; Peacock, A. J.; Mandelkern, L. *Macromolecules* **1989**, *22*, 3600.

31. Davison, W. H. T.; Corish, P. J. *J. Chem. Soc.* **1955**, 2428.

32. VanderHart, D. L. *J. Mag. Res.* **1981**, *44*, 117.

33. Yamanobe, T. In Solid state NMR of polymers; Ando, I.; Asakura, T. (Eds.); *Studies in Physical and Theoretical Chemistry* **1998**, *84*, 267.

34. Bunn, C. W. *Trans. Faraday Soc.* **1939**, *25*, 482.

35. Ward, I. M.; Sweeney, J. In An introduction to the mechanical properties of solid polymers 2nd edition; John Wiley & Sons Ltd: Chichester, **2004**; p. 273.

36. Myers, T. N. In Encyclopedia of polymer science and technology 3rd edition, Mark, H. F. (ed.); John Wiley & Sons: Hoboken NJ, **2005**; p. 569.

37. Jose, J.; Li, S.; Bouzidi, L.; Leao, A. L.; Narine, S. S. *J. Appl. Polym. Sci.* **2014**, *131*, 40492.